15TH IEA HEAT PUMP CONFERENCE
MAY 26–29, 2026 | HOFBURG
VIENNA 2026
DECARBONISATION THROUGH INNOVATION

From ground source heat pump monitoring to modelling of temperature field around borehole heat exchangers

Mahaut Magin[a,b,*], Bertrand François[b], Pierre Gerard[a]

[a] Université libre de Bruxelles (ULB), Building, Architecture and Town Planning Dept (BATir), GeoMechanics Laboratory, Avenue F.D. Roosevelt, 50 - CPI 194/2, B-1050 Bruxelles, Belgium
[b] Université de Liège (ULiège), Urban and Environmental Engineering Dept (UEE), Allée de la Découverte, 9 - 4000 Liège, Belgium

Abstract

Closed-loop and vertical Borehole Heat Exchangers (BHEs) are a common solution adopted for shallow geothermal energy systems. However, during the operational life of such systems, the evolution of subsurface temperatures is rarely monitored. As a result, Ground Source Heat Pump (GSHP) settings are typically adjusted solely based on the building's heating and cooling demands, without considering the thermal state of the ground. This can lead to either depletion of the ground heat reservoir and reduced system performance over seasonal cycles or under-exploitation of available thermal resources, representing a missed opportunity in terms of return on investment.
This study demonstrates how long-term monitoring of a residential GSHP installation can be used to assess the performance of the system, to identify operational patterns, and to evaluate the sustainability of its interaction with the subsurface. Four years of inlet and outlet fluid temperatures, flow rates, and electricity consumptions were collected at the GSHP of a Belgian single-family house equipped with one 107 m deep BHE. These data were processed to distinguish operating modes, analyze the seasonal evolution of the borehole fluid temperature, quantify extracted and injected heat according to the operating modes, and compute performance indicators.
In addition to the monitoring analysis, a preliminary modelling exercise was carried out using an existing analytical heat transfer model for BHEs based on g-functions for finite line source model. The monitored heat load extracted or injected in the ground was used as input, and simulated fluid temperatures were compared with measurements to explore the potential of such modelling for future calibration and predictive applications. While not intended as a fully validated predictive tool in this study, this first comparison illustrates how combining monitoring data with heat transfer models could ultimately support more informed and sustainable operational strategies.

Keywords: Borehole heat exchanger; Ground source heat pump; Monitoring; System performance; Heat transfer modelling

1. Introduction

When considering shallow geothermal energy systems for heating and cooling buildings, closed-loop vertical Borehole Heat Exchangers (BHEs) are often used because of their implementation flexibility. They can be installed in most locations and typically require less costly preliminary studies than open-loop systems (i.e., geothermal wells), making them a promising solution for urban deployment. During the design phase of such systems, a series of assumptions are made regarding the thermal properties of the ground and the heating and cooling demands to be met by the system. However, once the system becomes operational, the Ground Source Heat Pump (GSHP) settings are selected and subsequently adjusted throughout the system's lifetime, often without considering the thermal state of the ground. If the ground's thermal properties were overestimated and/or the building demand underestimated, the ground heat reservoir will gradually deplete, leading to a decline in system performance. Conversely, if the system is oversized or the thermal demand is overestimated, the available thermal resources will not be fully exploited. Although this situation is less critical

* Corresponding author.
E-mail address: mahaut.magin@ulb.be

15th IEA Heat Pump Conference 2026 - IGS5.1 - https://doi.org/10.23697/0es1-pg38

in terms of performance degradation, it results in inefficient use of the subsurface potential. Implementing monitoring devices is thus essential to prevent such issues and ensure a more sustainable operation of the system.

Most closed-loop geothermal systems consist of multiple BHEs [1-2], which together form geothermal bore fields. Large geothermal bore fields tend to be more frequently monitored [3-5] than smaller systems, as the cost of monitoring is more easily offset in large systems due to their higher economic impact. As a result, such small systems [6] are largely underrepresented in monitoring studies. Yet, assessing the long-term performance of smaller systems is equally important. Evaluating their efficiency can help promote their adoption among private homeowners and ultimately increase their number. For both small and large systems, monitoring data can be used to support more sustainable management of the underground heat reservoir through performance analyses and heat transfer simulations.

The primary parameters to monitor are the inlet and outlet temperatures in the geothermal loop, corresponding to the fluid entering and leaving the GSHP. This information alone already allows to analyze the evolution of the fluid temperature in the geothermal loop [3-5,7-8], whether over seasonal cycles or through more dynamic, short-term variations. Seasonal cycles analysis makes it possible to detect a potential depletion of the ground heat reservoir, suggesting that the system is undersized. Secondly, by measuring the flow rate in that loop, the thermal power and the energy extracted from or injected into the ground can be computed, typically using a heat meter [3,5-9]. Similar monitoring devices can also be installed on the loops connecting the GSHP to the building to quantify the thermal energy delivered for space heating, domestic hot water (DHW), and cooling. Thirdly, the electrical consumption of both the GSHP and the circulating pumps in the different loops can be recorded in order to determine the total electrical consumption of the system. Combining these measurements enables an accurate assessment of the energy performance of the installation [3,6-9]. The different sensors and meters presented above can be implemented either during the initial construction phase or retrofitted afterwards.

To obtain more detailed information on the temperature around or within the BHE(s) at different depths, temperature sensors such as optical fibers can be installed in the geothermal grout or within the geothermal pipes [7-8]. However, this type of monitoring is far from straightforward. The installation of such fragile sensors is technically demanding and requires careful coordination with the drilling team. Moreover, when installed in the grout, the distance between the sensor and the pipes is uncertain and may vary along the depth, which is why processing and interpreting vertical temperature profiles requires substantial expertise. While these measurements alone do not allow direct assessment of system efficiency, they provide high-resolution insight into the evolution of subsurface temperatures. This is particularly valuable for identifying potential depletion of the heat reservoir (or of specific layers within it) and for calibrating heat transfer models [4-5,7].

This study focuses on the energy performance analysis of a single-BHE system, based on four years of monitoring data collected at the GSHP (temperatures and flow rates in the different loops, as well as electrical consumptions). This geothermal system supplies heating and cooling to a Belgian single-family house. The paper also discusses monitoring data processing and interpretation in the light of seasonal needs of the building and its occupants. Furthermore, the heat load derived from the monitored data is used as input for an existing analytical model of heat transfer between the BHE and the ground. Preliminary simulation results based on estimated geothermal properties are presented and discussed.

2. Case study description

The single-family house investigated in this study is located in Brussels, Belgium. Its construction was completed in October 2012. The building has a total floor area of 306 m², with an annual energy consumption predicted by the pre-construction energy assessment of 14 kWh/m². It is equipped with a closed-loop shallow geothermal system consisting of a GSHP with a nominal capacity of 7.74 kW and a single BHE. The borehole, filled with thermal grout, has a length of 107 m and a diameter of 130 mm. The geology crossed by the borehole consists of a succession of horizontal layers corresponding to Cenozoic sedimentary deposits, alternating between sands and clays. The circulating pipe, which carries an antifreeze solution composed of 25% monopropylene glycol and 75% water, is configured as a double U-tube with an outer diameter of 32 mm.

The system provides energy for space heating through a radiant floor system and for DHW production. During summer, the GSHP can be bypassed, allowing for passive cooling through a plate heat exchanger.

In 2020, an external monitoring system was installed on the operating installation. As illustrated in Fig. 1, this system measures the fluid temperatures in the geothermal loop entering the GSHP T_1 and exiting it T_2; in the DHW loop leaving T_3 and returning T_4 to the GSHP; and in the floor heating loop leaving T_5 and returning

T_6 to the GSHP. The DHW and floor heating setpoint temperatures are 52 °C and 40 °C, respectively. Volumetric flow meters record the flow rates in each loop (Q_1 for the geothermal loop, Q_3 for the DHW loop, and Q_5 for the floor heating loop). Additionally, electricity meters monitor the power consumption of the circulating pumps (Cel_1, Cel_3 and Cel_5) and of the GSHP unit itself Cel_7.

All data from these sensors and meters are logged every 15 minutes. The present analysis focuses on four years of monitoring data, covering the period from September 2020 to August 2024.

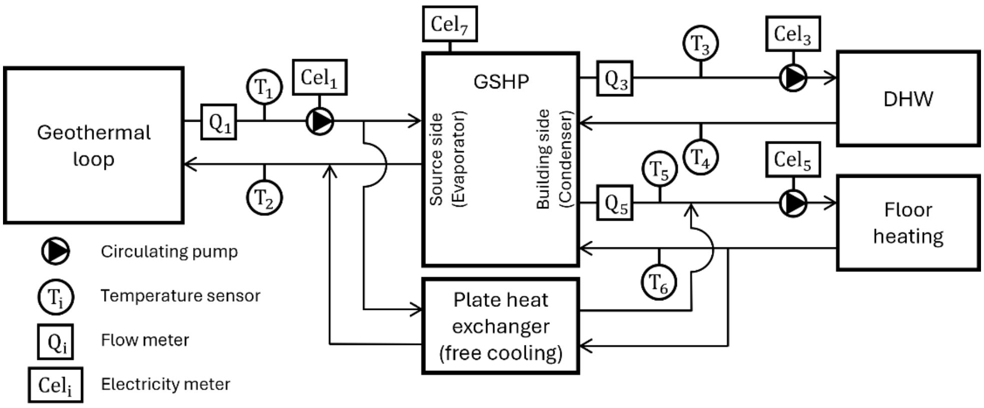

Figure 1. External monitoring system.

3. Energy performance of the system

3.1. Data processing

The raw data recorded every 15 minutes includes the temperatures at the inlet and outlet of the GSHP in the different loops, the cumulative water volume circulating through each loop, and the electrical consumption of the system.

To analyze the energy performance of the system, it is first necessary to define precisely the operating state of the system at each time step; specifically, whether the system is off or running, and if running, under which operating mode (heating, DHW, or free cooling). The most reliable way to determine this is to use the flow rates measured by the volumetric counters (Q_1, Q_3 and Q_5, in m^3/15 min). The operating modes are defined as follows:

- The system operates in DHW mode if $Q_1 > 0$ and $Q_3 > 0$
- The system operates in heating mode if $Q_1 > 0$ and $Q_5 > 0$
- The system operates in free cooling mode if $Q_1 > 0$ and $Q_3 = Q_5 = 0$ (since the volumetric counter Q_5 is bypassed in this case)

If none of these conditions are met, the system is considered off.

It is important to note that simultaneous operation of two modes is not possible; nonetheless, successive operation of different modes may occur within a 15-minute timeframe. Furthermore, since a mode may begin or end partway through a 15-minute interval, it is essential to identify the precise operating time of each mode within that interval. Since each loop has a constant flow rate (a parameter that is not adjusted by the GSHP), the volume of water circulating over 15 minutes Q_t is known. The real operating time Δt_{op}, expressed in hours, in each time interval can be determined from the ratio between the measured volume during the interval Q and the total possible volume for 15 minutes Q_t:

$$\Delta t_{op} = \frac{Q}{4Q_t} \quad (1)$$

By filtering the operating modes based on flow rate, only the periods when the GSHP is actually running are considered. This approach ensures that temperature readings used in the energy performance analysis are not affected by ambient indoor conditions (as it is the case when no circulation occurs in a loop) or by the operation of other loops, leading to a more accurate assessment of the system's energy performance.

The thermal power extracted from the ground can be calculated for every 15-minute interval as:

$$P_E = \rho_f c_{p,f} Q_1 (T_1 - T_2) \quad (2)$$

where $\rho_f c_{p,f}$ is the volumetric heat capacity of the circulating fluid (i.e., 25% monopropylene glycol and 75% water in the geothermal loop), taken as 4 MJ/(K·m³). During summer, when the free cooling mode is active, this power takes a negative value.

The extracted power can then be decomposed according to the three operating modes. If only one mode is active during the 15-minute interval, the calculated power is assigned entirely to that mode. However, if two modes are active successively within the same interval, the power is distributed proportionally according to their respective operating times (i.e., based on the ratio between the operating time of the considered mode and the total system operating time over that interval).

The thermal power supplied to the house for both heating and DHW was not computed, as the temperatures T_3 to T_6 exhibited values inconsistent with the operating state of the heat pump and with the fluid temperature in the geothermal loop, and could therefore not be used reliably for such calculations.

The energy exchanged over a given period of n times 15 minutes is obtained by performing a discrete integration of the thermal power extracted during each 15-minute interval (Eq. 2) multiplied by the actual operating time Δt_{op} within that 15-minute interval (Eq. 1). This allows determining the total energy injected or extracted from the ground over the selected period:

$$E = \sum_{i=1}^{n} P_{E,i} \Delta t_{op,i} \quad (3)$$

Finally, the Coefficient of Performance (COP) of the system can be determined. By definition, the COP is the ratio between the thermal power delivered to the building (for both heating and DHW) and the total electrical power consumed by the system P_{elec}.

In this study, since the thermal power delivered to the building could not be accurately calculated, an alternative approach was adopted. Based on the power balance derived from the first law of thermodynamics applied to the heat pump, the thermal power supplied to the building is assumed to be equal to the sum of the thermal power extracted from the ground P_E and the electrical power supplied to the heat pump P_{HP}, multiplied by the heat pump's efficiency (η = 98%, considered high since the thermal exchanges occur entirely within its sealed casing):

$$COP = \frac{(P_E + P_{HP})\eta}{P_{elec}} \quad (4)$$

This equation can then be applied separately for each mode (heating and DHW) by using the extracted power and electrical consumption recorded while the corresponding mode was active, thereby allowing the COP of the system in each specific mode to be determined.

3.2. Results interpretation

As explained in the previous section, when the system is not operating, the temperature sensors located near the heat pump record the indoor ambient temperature rather than the actual temperature of the circulating fluid. Moreover, due to the thermal inertia of the installation, the fluid requires more than ten minutes to complete a full circulation through the geothermal loop. Consequently, the temperatures recorded at the beginning of each operating period do not correspond to the actual fluid temperature within the borehole. For these reasons, a data filtering process was applied to retain only the inlet and outlet temperatures that reliably represent the temperature of the fluid circulating in the ground loop.

The evolution of the inlet and outlet fluid temperatures in the geothermal loop after filtering, as well as their difference, is presented in Fig. 2. Firstly, the fluid temperature remains within an acceptable range [0 – 20 °C] all along the monitored period. Secondly, when the heat pump operates in steady state (in both heating and DHW modes), the difference between the inlet and outlet temperatures remains nearly constant (around 3.5 °C), indicating that the electrical power supplied to the GSHP is the main factor controlling the thermal power delivered to the building. In contrast, when the GSHP is bypassed for free cooling, the temperature difference varies between –1 and –6 °C. When this mode is active, cooling is achieved through direct heat exchange between the floor heating loop and the colder geothermal loop via a plate heat exchanger. The initially large temperature difference leads to a high heat transfer rate, which decreases over time, thereby explaining the observed range of temperature differences. Finally, after each winter-summer cycle, the temperature returns to its initial value. This behavior suggests that the system is adequately sized and that no long-term thermal depletion of the ground is occurring. Because of this stable seasonal recovery, the late start of monitoring in 2020 (eight years after commissioning) does not compromise the analysis. The available dataset can therefore be confidently used for comparison with the simulation results presented later.

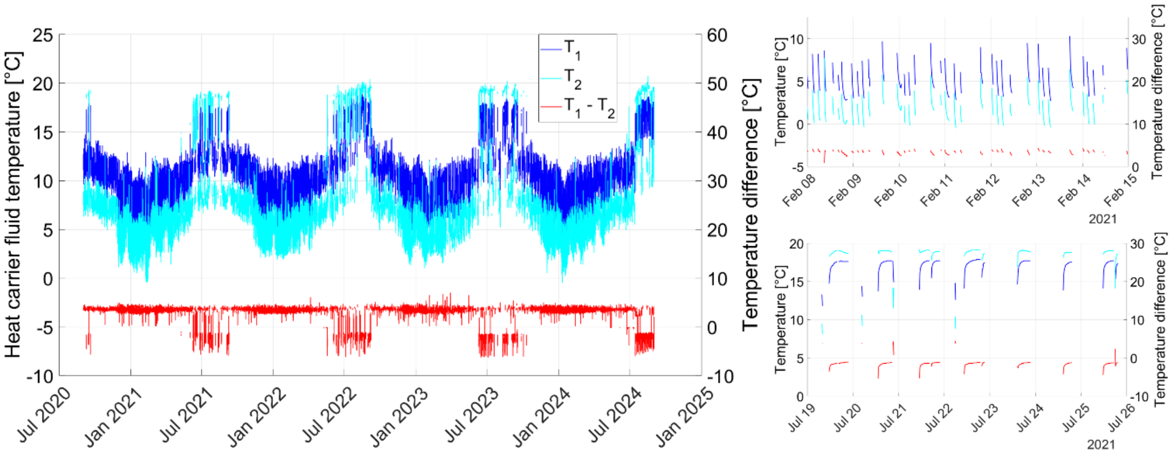

Figure 2. Evolution of the inlet and outlet fluid temperatures in the borehole and the difference between the two from September 2020 to August 2024, with a zoom on two specific weeks to visualize the evolution in detail.

The monthly energy injected or extracted from the ground for the three operating modes of the system between September 2020 and August 2024 is shown in Fig. 3. The energy extracted for space heating (in red) exhibits considerable differences between the first and second winters. These variations could be related to adjustments made to the GSHP settings by the occupants in reaction to the energy crisis, as reported by the property owner.

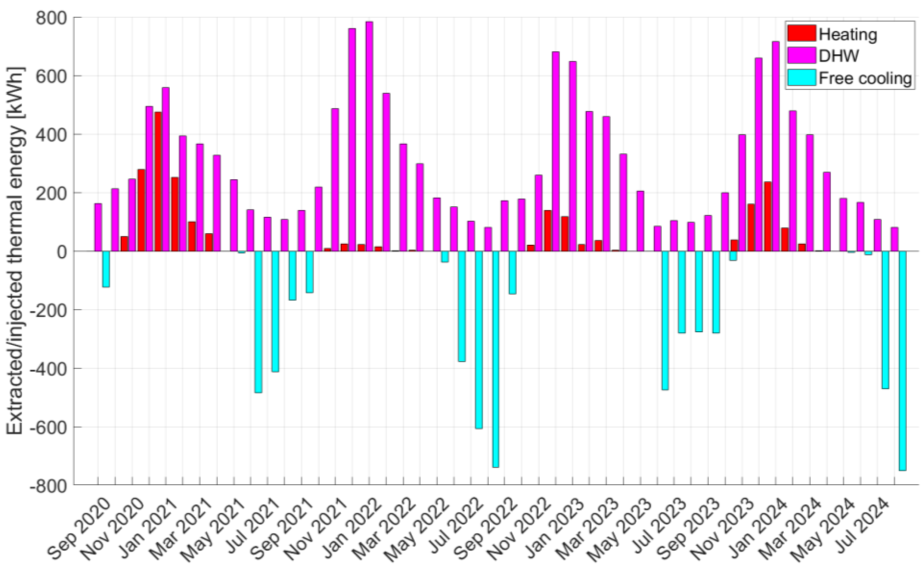

Figure 3. Monthly thermal energy extracted from or injected into the ground from September 2020 to August 2024.

The energy extracted for DHW (in purple) fluctuates from month to month, particularly between winter and summer periods, although the same seasonal trends repeat each year. This can be explained by the fact that during DHW production, the water flowing from a tap is a mixture of cold mains water and hot water stored in the buffer tank. In winter, the mains water temperature is lower than in summer, so a larger amount of hot water is required to reach the desired tap temperature. Moreover, showers tend to be longer and hotter in winter. The combination of these two effects explains the intra-annual variations observed in the DHW energy demand.

In summer, thermal energy is injected into the ground for free cooling (in blue), mainly between June and September. Although the amount of injected energy is lower than the energy extracted during the heating season, it remains sufficient to ensure an effective seasonal regeneration of the ground. This summer recharge contributes to restoring the thermal balance of the subsurface and prevents long-term thermal depletion of the heat reservoir.

The monthly COP of the system for both heating and DHW modes over the four years of monitoring are shown in Fig. 4. It is worth noting that, at the start of each operation cycle, the temperature difference between the inlet and outlet on the source side of the heat pump is generally small, resulting in higher electrical consumption and thus lower instantaneous performance. In other words, the system's performance during start-up is significantly lower than during steady operation. In the results presented here, entire operation cycles are considered, including transient phases, in order to determine the actual performance of the system under real operating conditions.

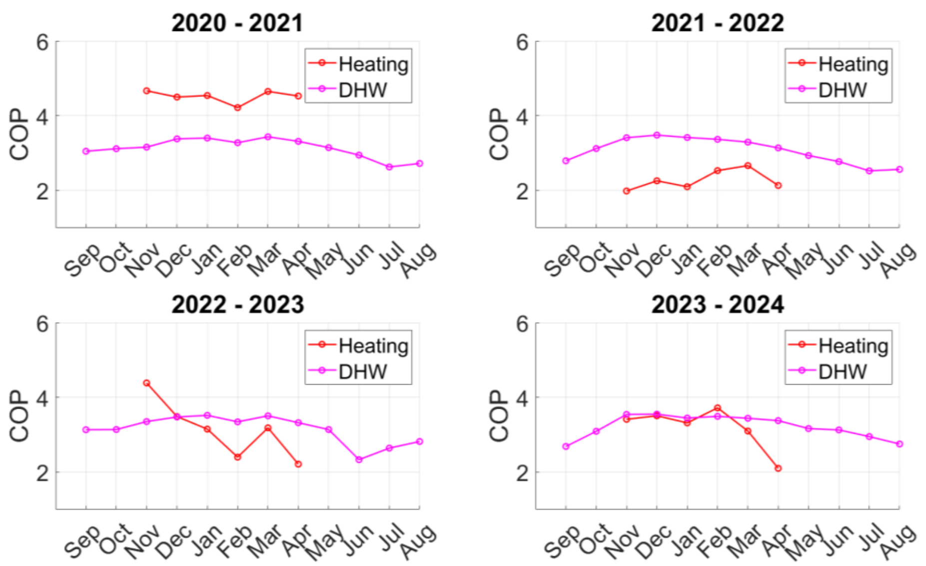

Figure 4. Monthly COP of the system over the four years of monitoring for both heating and DHW modes.

The COP in DHW mode remains consistent throughout the years and performs relatively well, with an average value above 3 (Fig. 4). Interestingly, the system tends to be slightly more efficient during winter, as it operates over longer continuous periods. This observation is illustrated in Fig. 5, where the DHW operating periods recorded in July 2021 are noticeably shorter than those in January 2021, illustrating the reduced hot water demand and shorter run cycles during summer.

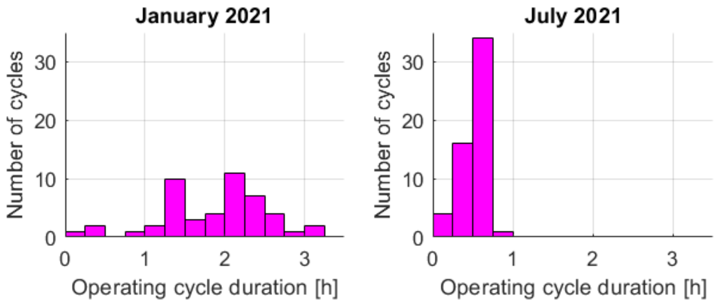

Figure 5. Histogram of DHW-cycle durations for one winter and one summer month (2021): total operating time [h] and number of start-ups — January: 89.3 h / 48 start-ups; July: 27.7 h / 55 start-ups.

In contrast, the COP in heating mode shows strong interannual variability (Fig. 4). It is excellent during the first year, with an average of 4.5, but drops sharply in the second year to an average of 2.3. This difference is directly linked to the changes in GSHP control settings between these two winters. The new configuration led to fewer start-ups and reduced operating time (Fig. 6), meaning that the GSHP operated mainly in transient conditions and rarely reached steady-state operation, which significantly reduced its performance. Nevertheless, these new settings also resulted in a substantial reduction in electrical consumption (from 356.6 kWh during the first winter to 61.5 kWh during the second), indicating a trade-off between energy efficiency and operational economy. During the third and fourth years, the situation is intermediate between those of the first two winters.

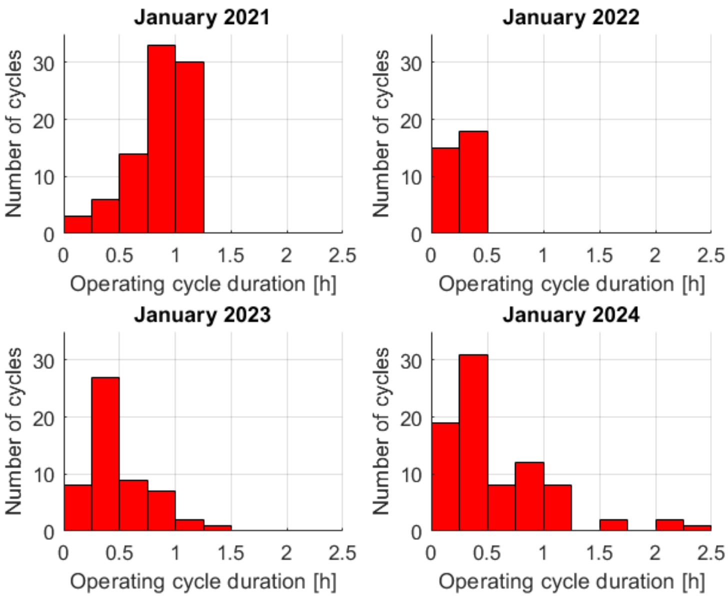

Figure 6. Histogram of heating-cycle durations for January over four heating seasons (2021 to 2024): total operating time [h] and number of start-ups — 2021: 73.3 h / 86 start-ups; 2022: 7.7 h / 33 start-ups; 2023: 26.7 h / 54 start-ups; 2024: 47.6 h / 83 start-ups.

Finally, the monthly energy extracted from the ground for heating is compared with meteorological data in order to better understand the relationship between climatic conditions and system performance. The meteorological data, including heating degree days and sunshine duration, were obtained from the Royal Meteorological Institute of Belgium, based on measurements from the Uccle observation station in Brussels (located at 8.6 km from the study house).

Heating degree days were calculated for each month as the sum of the differences between the reference temperature (15 °C) and the daily average temperatures, whenever the latter were below 15 °C. This indicator provides an estimate of the building's heating demand.

Given that this house is a very low-energy building with high solar exposure, it is also relevant to compare the monthly cumulative sunshine duration (in hours) with the energy extracted from the ground for heating purposes.

Fig. 7 presents this comparison for the winter of 2022–2023, showing the monthly energy extracted alongside the corresponding heating degree days and sunshine duration. A clear correlation can be observed between the amount of energy extracted from the ground and the heating degree days of each month. A similar trend appears with sunshine duration: months with lower sunshine duration generally correspond to higher amounts of energy extracted from the ground. These results confirm that climatic factors strongly influence the operation and performance of shallow geothermal systems, even at the single-BHE scale.

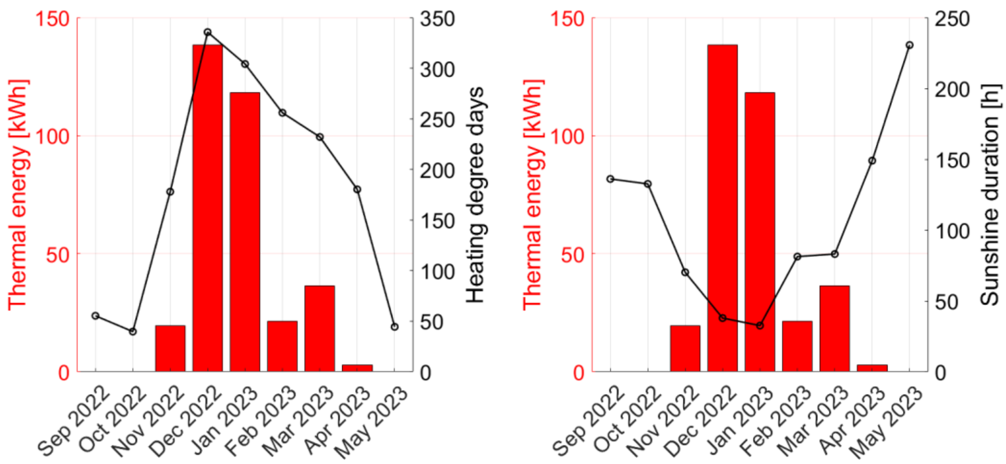

Figure 7. Monthly thermal energy extracted from the ground for heating compared with meteorological data during winter 2022-2023.

4. Modelling of subsurface heat transfer

In this section, an existing analytical heat transfer model is used to simulate the thermal response of the borehole. The monitored data, and in particular the extracted and injected thermal power, are exploited to define the time-dependent thermal load imposed on the ground during the simulation. The model is run using estimated geothermal properties representative of the local geological context. A preliminary comparison between the simulated fluid temperature and the mean measured temperature in the geothermal loop (Fig. 2) is then performed in order to assess the model's ability to reproduce the observed thermal behavior and to highlight its potential for future predictive applications and inverse analyses.

4.1. Model hypothesis

The model used in this study is an analytical ground heat transfer model previously developed by Erol et al. [10] and Coen et al. [11] to predict both the heat carrier fluid temperature and the surrounding ground temperature under dynamic heat extraction or injection loads. The latest version of this model accounts for conductive, advective, and dispersive heat transport in the subsurface around one or multiple BHEs. It also allows for the simulation of thermal interactions between several boreholes and for the implementation of time-dependent thermal loads, which can be defined independently for each BHE.

In the present study, however, the system consists of a single BHE, and groundwater flow is assumed to be negligible. As a result, heat transfer in the ground is governed solely by conduction, and the model reduces to the general heat transfer equation in a porous medium:

$$\rho_m c_{p,m} \frac{\partial T}{\partial t} = \lambda_m \left(\frac{\partial^2 T}{\partial x^2} + \frac{\partial^2 T}{\partial y^2} + \frac{\partial^2 T}{\partial z^2} \right) + s \tag{5}$$

where $\rho_m c_{p,m}$ is the volumetric heat capacity of the ground, λ_m its thermal conductivity (assumed homogeneous and isotropic), and s the volumetric heat source term.

A g-function based analytical solution of this partial differential equation denoted f(x,y,z,t) has been developed for a finite line source representing the borehole. To account for time-varying thermal loads $q_L(t)$, the temperature evolution ΔT at any point is obtained by time convolution of the load history:

$$\Delta T(x,y,z,t) = \sum_{i=1}^{n} q_L(i\Delta t) f(x,y,z,t-(i-1)\Delta t)\Delta t \tag{6}$$

where n is the number of time steps Δt considered in the simulation.

The average temperature of the circulating fluid T_f can be derived from the temperature variation at the borehole wall, $\Delta T(r = r_b)$, by simplifying the heat transfer dynamics within the borehole to a single thermal resistance R_b, according to:

$$T_f = T_g + \Delta T(r = r_b) + R_b q_L \tag{7}$$

where T_g is the initial undisturbed ground temperature and r_b is the borehole radius.

Finite line source-based g-functions are suitable only for long-term predictions (> ~5-10h according to Eskilson [12]), as they neglect transient thermal effects within the BHE, which are represented by a simple thermal resistance. Based on the thermal response time of the system, steady-state heat transfer within the borehole is reached after approximately one hour, which therefore defines a lower limit for the temporal resolution of the applied thermal load. Although full time-scale simulation models exist in the literature, combining, for example, thermal resistance–capacitance models for short-term transient heat transfer within the BHE with g-functions for long-term heat transfer in the surrounding ground [13], the present modelling approach is well suited for first-order predictions and for comparison with monitoring data. Given the time scale considered in this study, this approach provides a satisfactory representation of the borehole thermal behavior.

The input load q_L provided to the model corresponds to the thermal power extracted from or injected into the ground (in W/m). This load can be directly computed from the monitored thermal power data of the GSHP system (Eq. 2). A negative load indicates heat extraction (heating mode or DHW mode), while a positive load represents heat injection (free cooling).

For the simulation, subsurface thermal properties were estimated using a lithology-based thermal conductivity model informed by regional geological data for Brussels [14-15]. The borehole thermal resistance was derived from the borehole geometry [16], assuming a grout thermal conductivity of 1.6 W/(m·K). The parameters used are summarized in Table 1.

Table 1. Estimated subsurface thermal properties

Geological parameters	Estimated values
Initial ground temperature T_g	12.5 °C
Ground thermal conductivity λ_m	1.9 W/(m·K)
Ground volumetric heat capacity $\rho_m c_{p,m}$	2.7 MJ/(m³·K)
Borehole thermal resistance R_b	0.081 m·K/W

4.2. Results and discussion

Fig. 8 shows the evolution of the simulated circulating fluid temperature obtained by applying the thermal load derived from the monitoring data. The original thermal load, recorded at 15-minute intervals, was averaged to an hourly resolution to satisfy the assumptions of Eq. 7. On the other hand, the time step used to compute the temperature evolution (Eq. 6) is set to 15 minutes so as to match the discretization of the monitored temperatures. Knowing that this simulation consists exclusively in blind prediction, based on expected thermal characteristics of the ground, without any parameter calibration, the modelling results compare very well with monitoring data. The simulation reproduces the same overall trend and a comparable order of magnitude as the measured data. Nevertheless, significant improvements are needed to reduce discrepancies, particularly noticeable during winter.

First, the subsurface thermal properties and borehole thermal resistance (Tab. 1) could be calibrated more accurately, for instance using specific inverse analysis techniques. Moreover, the study compares monitored and predicted fluid temperatures at 15-minute intervals (Fig. 8), while an average hourly thermal load is imposed to satisfy the steady-state heat transfer requirements within the borehole (Eq. 7). This approach cannot fully capture the transient dynamics of the system. To address this limitation, enhancements to the existing analytical heat transfer model could be considered by integrating short-term effects within the borehole into the long-term framework based on g-functions, improving predictions of transient variations in the heat carrier fluid temperature [13].

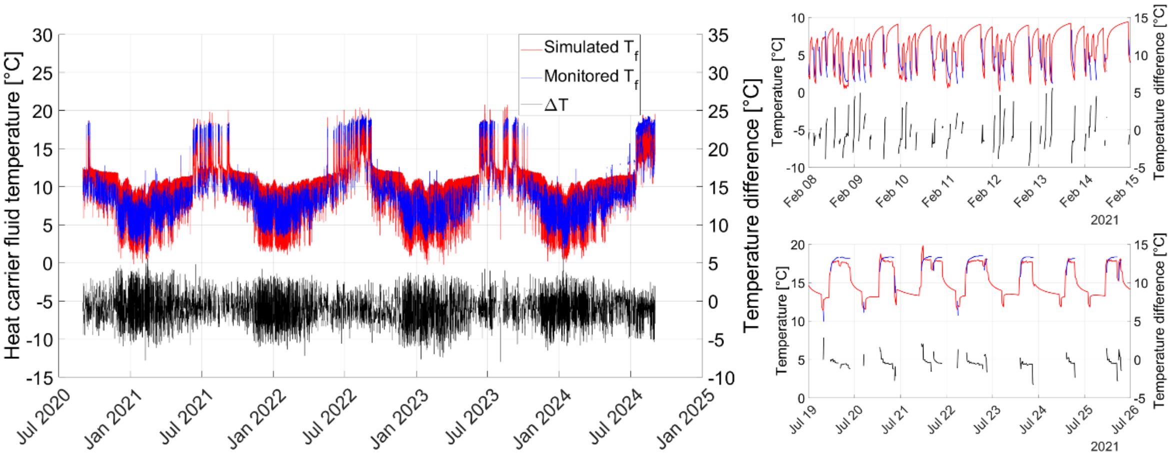

Figure 8. Evolution of the simulated and monitored circulating fluid temperature and the difference between the two from September 2020 to August 2024, with a zoom on two specific weeks to visualize the evolution in detail.

5. Conclusion

This study highlights the importance of high-quality monitoring for understanding and optimizing the performance of shallow geothermal systems. Using flow rate measurements allows to distinguish the operating modes of the GSHP and can lead to refined analysis of the performance of the system according to the operating mode. The processed data revealed clear seasonal trends, consistent recovery of the subsurface temperature after each annual cycle, and meaningful differences in system performance between heating and DHW modes. These observations confirm not only that the installation is correctly sized, but also that long-term monitoring can capture the impact of operational choices on system efficiency.

Building on these results, this study demonstrates that analyzing the performance of a shallow geothermal system based on detailed monitoring data provides valuable insight into the thermal behavior of the subsurface. Such an approach makes it possible not only to assess the energy efficiency of the installation but also to infer the thermal state of the ground. In practice, this information could be used to adjust the operating settings of the GSHP according to the thermal conditions of the subsurface, rather than solely on the instantaneous heating or cooling demand. This would contribute to a more sustainable and balanced use of the underground thermal reservoir over time.

Future developments should focus on the implementation of inverse modelling methods to refine the estimation of subsurface and BHE thermal properties. This would enable a more accurate characterization of the subsurface and improve the reliability of the model calibration. Once properly calibrated, the analytical model could be used to perform predictive simulations of the ground temperature evolution under various operating and climatic scenarios, helping to optimize system performance over its lifetime.

The methodology and workflow developed in this study are not limited to single-BHE installations. They can be extended to more complex systems such as BHE fields, where interactions between boreholes and temporal variations in load distribution play a significant role.

Acknowledgements

This work was supported by the Walloon Region, and especially the SPW Economy, Employment, Research and the Walloon Recovery Plan in the frame of the research project n°2310143 "Enhanced Flexibility in Energy Systems (EFES)".

References

[1] Lund JW, Boyd TL. Direct utilization of geothermal energy 2015 worldwide review. *Geothermics* 2016;60:66–93. DOI: 10.1016/j.geothermics.2015.11.004.

[2] Gao Q, Li M, Yu M, Spitler JD, Yan YY. Review of development from GSHP to UTES in China and other countries. *Renewable Sustainable Energy Rev* 2009;13(6):1383–94. DOI: 10.1016/j.rser.2008.09.012.

[3] Bockelmann F. IEA HPT Annex 52 – Long-term performance monitoring of GSHP systems for commercial, institutional and multifamily buildings: Case study report for KON, Germany. In: *IEA HPT Annex 52 – Long-term performance monitoring of GSHP systems for commercial, institutional and multifamily buildings*; 2021. DOI: 10.23697/19wq-wn21.

[4] Heim E, Stoffel P, Müller D, Klitzsch N. Six years of high-resolution monitoring data of 40 borehole heat exchangers. *Sci Data* 2024;11:1334. DOI: 10.1038/s41597-024-04241-9.

[5] Naicker SS, Rees SJ. Long-term high frequency monitoring of a large borehole heat exchanger array. *Renew Energy* 2020;145:1528–42. DOI: 10.1016/j.renene.2019.07.008.

[6] Stafford A. Long-term monitoring and performance of ground source heat pumps. *Build Res Inf* 2011;39(6):566–73. DOI: 10.1080/09613218.2011.603599.

[7] Montagud C, Corberán JM, Montero Á, Urchueguía JF. Analysis of the energy performance of a ground source heat pump system after five years of operation. *Energy Build* 2011;43(12):3618–26. DOI: 10.1016/j.enbuild.2011.09.036.

[8] Piscaglia F, Blasi A, Del Moro S, Polonara F, Arteconi A, Zanarelli L, Renzulli A. Monitoring of a vertical borehole ground-coupled heat pump system: A case study from a marly-limestone heat reservoir (Urbino, Central Italy). *Geothermics* 2016;62:61–9. DOI: 10.1016/j.geothermics.2016.02.008.

[9] Han C, Yu X (Bill). Performance of a residential ground source heat pump system in sedimentary rock formation. *Appl Energy* 2016;164:89–98. DOI: 10.1016/j.apenergy.2015.12.003.

[10] Erol S, François B. Multilayer analytical model for vertical ground heat exchanger with groundwater flow. *Geothermics* 2018;71:294–305. DOI: 10.1016/j.geothermics.2017.09.008.

[11] Coen T, François B, Gerard P. Analytical solution for multi-borehole heat exchanger fields including discontinuous and heterogeneous heat loads. Energy Build 2021;253:111520. DOI: 10.1016/j.enbuild.2021.111520.

[12] Eskilson P. Thermal analysis of heat extraction boreholes. PhD thesis, Department of Mathematical Physics, University of Lund; 1987.

[13] Laferrière A, Cimmino M, Picard D, Helsen L. Development and validation of a full-time-scale semi-analytical model for the short- and long-term simulation of vertical geothermal bore fields. *Geothermics* 2020;86:101788. DOI: 10.1016/j.geothermics.2019.101788.

[14] Gerard P, Vincent M, François B. A methodology for lithology-based thermal conductivities at a regional scale for shallow geothermal energy – Application to the Brussels-Capital Region. *Geothermics* 2021;95:102117. DOI: 10.1016/j.geothermics.2021.102117.

[15] Centre Scientifique et Technique de la Construction (CSTC). Note d'information technique n°259 : Géothermie peu profonde – Conception et mise en œuvre de systèmes avec échangeurs en forme de U. 2016.

[16] Claesson J, Javed S. Explicit multipole formulas and thermal network models for calculating thermal resistances of double U-pipe borehole heat exchangers. *Sci Technol Built Environ* 2019;25(8):980–92. DOI: 10.1080/23744731.2019.1620565.